Pressure-induced phase transition, metallization, and superconductivity in boron triiodide

Nozomu Hamaya,[1,*] Miyuki Ishizuka,[1] Suzue Onoda,[1,2] Jiang Guishan,[1] Ayako Ohmura,[1,3] and Katsuya Shimizu[2]
[1]*Graduate School of Humanities and Sciences, Ochanomizu University, 2-1-1 Ohtsuka, Bunkyo-ku, Tokyo 112-8610, Japan*
[2]*KYOKUGEN, Center for Quantum Science and Technology under Extreme Conditions, Osaka University, 1-3 Machikaneyama-cho, Toyonaka, Osaka 560-8531, Japan*
[3]*Center for Transdisciplinary Research, Niigata University, 8050 Ni-no-cho, Nishi-ku, Niigata 950-2181, Japan*
(Received 29 May 2010; revised manuscript received 15 August 2010; published 7 September 2010)

Pressure evolution of structural and electrical properties of boron triiodide, a highly anisotropic molecular crystal consisting of stacked layers of planar BI_3 molecules, has been studied by x-ray diffraction and resistivity measurements. A new phase transition was observed to occur at 6.2 GPa from the molecular phase with hexagonal structure to a monatomic phase with the face-centered-cubic lattice of iodine atoms. This first-order phase transition is characterized by the discontinuous crush of stacking of molecular layers. The monatomic phase becomes metallic at ~23 GPa and exhibits superconductivity above ~27 GPa. The process of molecular dissociation and electrical properties of BI_3 are discussed in comparison with those of iodine and other simple molecular iodides.

DOI: 10.1103/PhysRevB.82.094506 PACS number(s): 62.50.−p, 61.05.cp, 31.70.Ks, 61.50.Ks

I. INTRODUCTION

The effect of high pressure on molecular systems has been a central issue of fundamental physics and chemistry[1] as well as planetary sciences.[2] Cohesion of simple molecular solids occurs through forces of very different strengths: covalent, ionic, van der Waals, and hydrogen bonds. Pressure drives materials to states of higher density and gives rise to competition among those chemical bonds, structural instabilities, and changes in electronic properties. A simple picture suggests that all molecular systems must collapse on compression to form closed-packed structures and go over into metallic states at sufficient high pressures.[3] However, the diversity of a process toward their destruction in real substances has manifested itself in numerous experimental observations. For instance, H_2 is widely known to exhibit unexpected phases and complex phase diagram.[4] Metal tetraiodides MI_4 (M=Ge,Sn) are examples of another class. They undergo pressure-induced amorphization[5–7] and become metallic glasses,[8] which are quite common in materials having tetrahedral coordination. Among various factors affecting on the response of molecular crystals to compression, the shape of a molecule may be of particular importance because the anisotropy of chemical bonds, crystal structure, and electronic properties strongly depends on the shape of molecules composing a crystal. In this study we experimentally investigate the pressure evolution of crystal structure and electrical resistivity of boron triiodide, a quasi-two-dimensional layered crystal consisting of planar molecules of BI_3. To our knowledge, a high-pressure study of molecular system having a simple planar molecule as a structural unit is quite rare.

The BI_3 molecule has a planer structure with the boron atom at the center of an equilateral triangle of the iodine atoms. The boron iodide crystallizes at ambient condition in an insulator having a hexagonal structure with space group $P6_3/m$.[9] Two molecules are included in the unit cell. Figure 1 shows the layered structure of BI_3, in which the planar molecules are arranged within the basal planes at $z=1/4$ and 3/4. A Raman spectroscopic measurement by Anderson and Lettress[10] showed no evidence of any phase transition or major distortion of molecules up to 5 GPa. Similar layered structures are found in quasimolecular iodides of the type MI_3 (M=As,Sb,Bi), although their crystal structures belong to the rhombohedral symmetry with space group $R\bar{3}$.[11] The molecular and ionic characters coexist in these iodides. Among them, the molecular character is well preserved in AsI_3 consisting of molecules with depressed triangular pyramid structure. It has been shown by x-ray diffraction and Raman spectroscopy that in AsI_3 the distinction between the

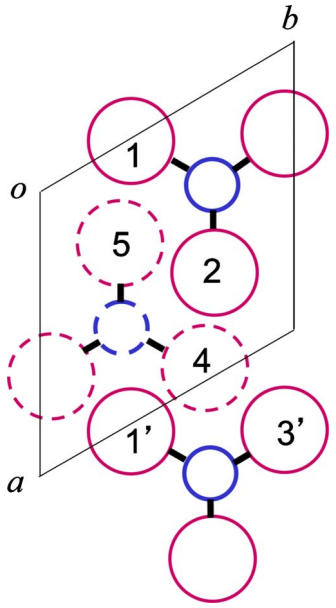

FIG. 1. (Color online) Hexagonal crystal structure of BI_3 with space group $P6_3/m$ projected on the xy plane. The boron atom (small circle) sits at the center of an equilateral triangle of the iodine atoms (large circle) in a molecule. Planar molecules lie perpendicular to the c axis at $z=1/4$ (solid line) and $z=3/4$ (broken line) and form a molecular layer at each height. Some iodine atoms are numbered for identification.

intramolecular and the intermolecular bonding is lost at ~4 GPa where the isostructural crossover from the molecular to the ionic crystal occurs.[12]

The purpose of this study is to investigate the response of highly anisotropic crystal structure consisting of planar molecules to compression. Choosing BI_3 as a planar molecular system, we have studied pressure-induced phase transition, molecular dissociation, metallization, and superconductivity by synchrotron and laboratory x-ray diffraction experiments and electric resistivity measurements. Results of Rietveld analysis provide detailed structural information concerning the approach to a phase transition and molecular dissociation. Metallization and superconductivity are explored over wide pressure and temperature ranges. The results for BI_3 are described in comparison with iodine and other simple molecular iodides with different shapes of molecules.

II. EXPERIMENTAL TECHNIQUE

A. X-ray diffraction study

Polycrystalline BI_3 of 98%+ purity obtained from Sigma-Aldrich Japan K. K. was ground into a fine powder. One sample out of three was prepared for synchrotron radiation (SR) x-ray diffraction study and the others for laboratory x-ray diffraction measurements. For the SR study a powder sample was placed into a hole of 0.17 mm diameter drilled in the T301 stainless steel gasket and loaded on a modified Mao-Bell-type diamond-anvil cell (DAC) with 0.6 mm culet anvils. For laboratory measurements two T301 gaskets with holes of 0.22 and 0.1 mm diameters were filled with the samples and loaded on membrane-type DACs with 0.6 and 0.3 mm culet anvils, respectively. A few ruby chips of 5–10 μm diameter were put in the hole together with the sample to determine the pressure by the ruby fluorescence method.[13] No pressure-transmitting medium was used. In the SR study average pressure distribution across the sample was measured to be ± 0.1 GPa at $P_{\text{average}}=3.7$ GPa, ± 0.2 GPa at 6.2 GPa and ± 0.3 GPa at 12.4 GPa and larger distribution amount to ± 0.5 GPa was often observed. Similar distribution was measured in the laboratory study below 4 GPa and at higher pressures the fluorescence from only a ruby chip could be detected. All the sample preparation was finished within 5 min in a globe box filled with cold nitrogen gas dried with pentaphosphourus oxide to avoid the reaction of the sample with water in air.

Synchrotron x-ray diffraction measurement was carried out up to 20 GPa at beamline BL04B2 in SPring-8. Incident x-rays at a wavelength of 0.3294 Å were collimated to 0.04×0.04 mm^2. An imaging plate was used as a detector. Acquisition time for each diffraction pattern was less than 1000 s. In the laboratory study x-rays from a rotating anode-type source with a molybdenum target were monochromatized by the pyroliticgraphite 002 reflection. Incident Mo$K\bar{\alpha}$ was collimated to 0.12 mm at the sample using a pin hole. Diffraction intensities were detected by an imaging plate with exposure times of 6–22 h. One sample was used to obtain diffraction patterns at low pressures below 10 GPa and they were analyzed by the Rietveld program of RIETAN-2000.[14] The other sample was compressed to 46 GPa. All measurements were done at room temperature.

B. Electrical resistivity measurement

A clump-type DAC made of nonmagnetic CuBe alloy was used to generate high pressure. Alumina powder was placed on the surface of a nonmagnetic 310S stainless steel gasket for electrical insulation. A sample was prepressed into dimensions of 40 μm thickness, 50 μm width and 100 μm length and embedded in the hole of insulated gasket. The electrical resistance was measured by an ac 4-terminal method with Pt electrodes with typical measuring current of 500 nA. The sample was treated in a water and oxygen-free argon gas glove box. The sample was compressed at room temperature and then cooled down to 60 mK by exploiting a ^{3}He/^{4}He dilution refrigerator. Pressure was determined by a ruby fluorescence method at low temperatures as well as at room temperature. Pressure gradient in the sample between electrodes was estimated to be less than 10% of the maximum pressure. Details of the technique have been described elsewhere.[15]

III. RESULTS

A. New phase transition

The SR measurement revealed a reversible drastic change in diffraction pattern around 7 GPa in the first pressure cycle. Figure 2 shows diffraction patterns recorded in the second compression. All of reflections observed below 6.4 GPa were indexed by the hexagonal symmetry with $P6_3/m$ space group, the structure reported at 1 atm. New peaks appeared at 7.0 GPa. With an increment of pressure they grew at the expense of the intensities of the hexagonal peaks, which finally disappeared at 9.1 GPa. More careful laboratory measurements demonstrated that this first-order phase transition occurred at 6.2 GPa and the reverse transition took place at 5.0 GPa.

A diffraction pattern of a high-pressure phase (HPP) can be well indexed with the face-centered-cubic (fcc) structure. The strongest peak corresponds to the 111 reflection. Since the atomic x-ray scattering power of boron is only 5/53 of that of iodine or less, we detect dominantly scattering from the iodine atoms. The present result indicates that the iodine atoms form the fcc lattice in the HPP. We did not see any signs of the presence of a super lattice structure: neither splitting of peaks nor appearance of additional peaks was observed in diffraction patterns of the HPP.

Rietveld refinement of the hexagonal structure was carried out to examine structural changes on approaching the phase transition. The space group of $P6_3/m$ was assumed in the analysis. In this structure the iodine atom has two independent positional parameters (x, y, 1/4) and the coordinate of the boron atom is fixed at (0, 1/3, 2/3). A typical result of Rietveld fitting is shown in Fig. 3. The R_{wp} factor to measure the degree of fit lied within a range of 5.1–6.8 % in the present analysis.

Figure 4 presents the results of pressure dependence of the lattice constants normalized to the values of those at 1

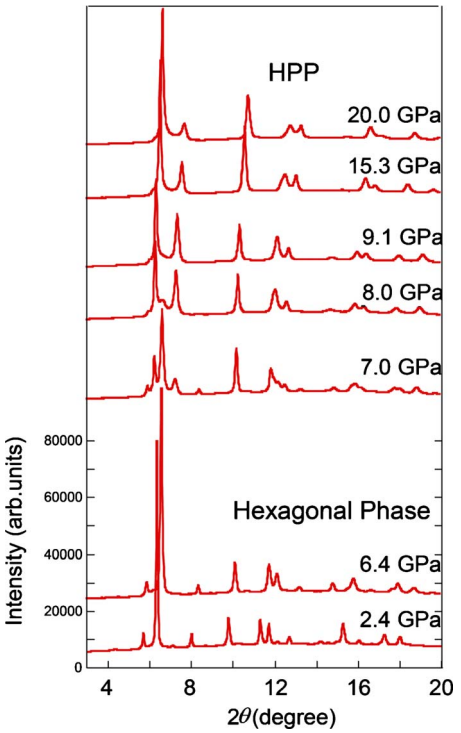

FIG. 2. (Color online) Pressure evolution of synchrotron x-ray diffraction patterns for BI_3 at $\lambda=0.32940$ Å on compression. Scattering from boron atoms must be invisible in diffraction intensities due to its low atomic scattering power in comparison with the iodine atom. A phase transition takes place at a pressure between 6.4 and 7.0 GPa in this run. Reflections from a HPP can be indexed with the fcc lattice.

atm, $a_0=6.9909$ Å and $c_0=7.3642$ Å. To clearly see anisotropic structural changes associated with the phase transition, the length scales of $a'/a_0=\sqrt{3/2}a_{\rm fcc}/a_0$ and $c'/c_0=(2/\sqrt{3})a_{\rm fcc}/c_0$ are plotted in the HPP region, where $a_{\rm fcc}$ is the lattice constant of the fcc lattice. A systematic discrepancy between the SR and the laboratory results is found in pressure dependence of the lattice constant c of the hexagonal phase. A possible cause may be the pressure gradient in the sample irradiated by x-rays. Pressure distribution across

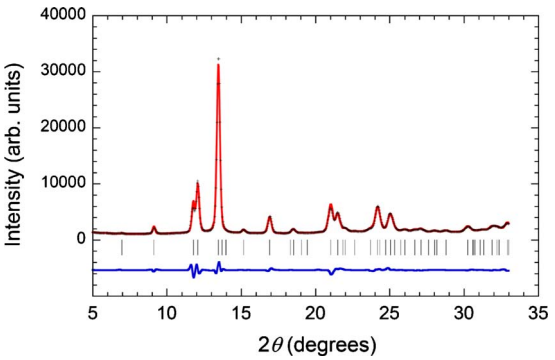

FIG. 3. (Color online) Result of Rietveld fitting of a typical diffraction pattern of the hexagonal phase at $\lambda=0.71073$ Å at 1.6 GPa. The space group of $P6_3/m$ was assumed. The boron atom was fixed at (0, 1/3, 2/3) and two independent positional parameters (x, y, 1/4) of the iodine atom were determined. $R_{\rm wp}$ was 5.1%.

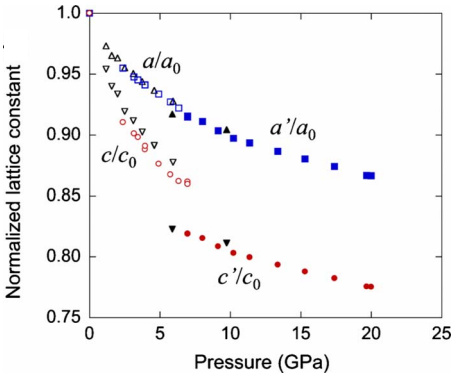

FIG. 4. (Color online) Pressure variations in the lattice constants a and c normalized to the values of those at 1 atm, a_0 and c_0. To clearly show anisotropic structural changes associated with the phase transition, the length scales $a'/a_0=\sqrt{3/2}a_{\rm fcc}/a_0$ and $c'/c_0=(2/\sqrt{3})a_{\rm fcc}/c_0$ are plotted in the HPP region, where $a_{\rm fcc}$ is the lattice constant of the fcc lattice. The SR data are denoted by a square for a and a circle for c and the laboratory data by a triangle for a and a reverse triangle for c. Open and solid symbols indicate the data for the hexagonal phase and the HPP, respectively.

the samples measured in this study has been described in chapter 2. Taking account of the beam size of x-rays, 0.04 mm-square and 0.12 mm diameter used in the SR and the laboratory study, respectively, the degree of discrepancy in c appears to be compatible with measured pressure distribution. Such an effect will be conspicuous in a more compressible direction as observed in the present case.

An important observation in Fig. 4 is that the stacking periodicity of molecular layers exhibits a discontinuous decrease by ~4% whereas the periodicity within the layer varies continuously across the transition point. The BI_3 molecule has such an electronic configuration that occupied p orbits of the iodine atoms and unoccupied p orbits of the boron atom elongate in the direction perpendicular to the molecular plane. Taking account of this electronic structure, we may consider that the shape of the BI_3 molecule is triangular prism and that the prisms are efficiently packed in the crystal structure of the molecular phase. Therefore the crush in the stacking direction clearly indicates break down of the molecules.

B. Compression curve

Measured volume per molecule is plotted as a function of pressure in Fig. 5. In the HPP region the volume per three iodine atoms $V_{\rm HPP}=(3/4)a_{\rm fcc}^3$ is plotted. The data were fitted to the Vinet equation of state[16] to obtain the bulk modulus at 1 atm K_0 and its pressure derivative K_0'. Least-squares analysis of the low-pressure phase yields $K_0=7.3\pm0.5$ GPa and $K_0'=7.0\pm0.5$ for the SR data and $K_0=7.8\pm0.3$ GPa and $K_0'=7.4\pm0.3$ for the laboratory data at a fixed volume of 155.85 Å^3/molecule at 1atm. They can be regarded to be in good agreement within experimental error. The value of the bulk modulus for BI_3 is compatible with $K_0=6.1$ GPa for SnI_4 (Ref. 17) and about a half of $K_0=13.6$ GPa for iodine.[18] A quasimolecular iodide of AsI_3 has a much larger value of

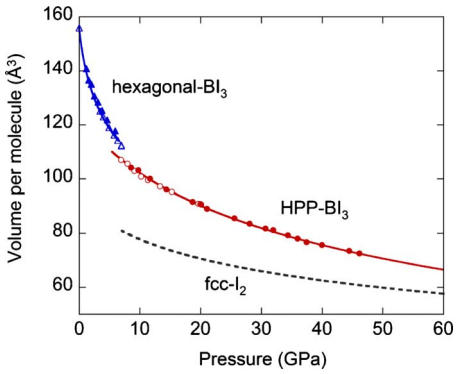

FIG. 5. (Color online) Measured volume per molecule plotted as a function of pressure. A triangle denotes the volume for the hexagonal structure. In the HPP region the volume per three iodine atoms $(3/4)a_{\mathrm{fcc}}^3$ (circle) is plotted. Open and solid symbols indicate the SR and the laboratory data, respectively. The Vinet fits to the experimental data are shown by solid curves: parameters used in the fits are $K_0=7.3$ GPa, $K_0'=7.0$, and $V_{0,\mathrm{hex}}=155.85$ Å^3/molecule for the hexagonal phase and $K_{0,\mathrm{HPP}}=41.0$ GPa, $K_{0,\mathrm{HPP}}'=3.0$, and $V_{0,\mathrm{HPP}}=123.0$ Å^3/three-iodine-atoms for the HPP. The dotted curve is an extrapolation of the equation of state for iodine with the fcc structure reported in Ref. 19 and shows $V=(3/4)V_{\mathrm{fcc-iodine}}$.

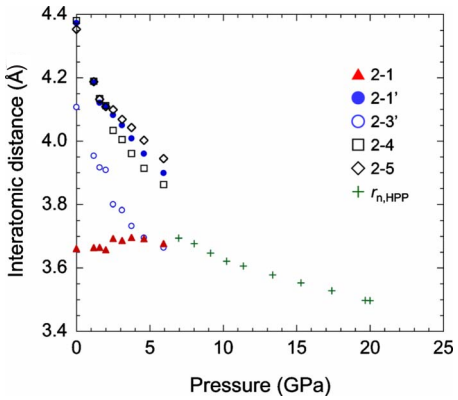

FIG. 6. (Color online) Pressure variation in interatomic distance r_{ij} between the ith and the jth iodine atoms. The numbers are shown in Fig. 1. The intramolecular distance is r_{21} (solid triangle). The intermolecular distances within the same molecular layer are $r_{21'}$ (solid circle) and $r_{23'}$ (open circle) and those between different layers are r_{24} (open square) and r_{25} (open diamond). The nearest-neighbor distance $r_n=a_{\mathrm{fcc}}/\sqrt{2}$ (cross) is plotted in the HPP region.

$K_0=62.5$ GPa (Ref. 12) due to coexisting ionic character of chemical bonds.

The HPP is much less compressible than the hexagonal phase. The fitting of all data for the HPP yields $K_{0,\mathrm{HPP}}=41.0\pm0.6$ GPa, $K_{0,\mathrm{HPP}}'=3.0\pm0.6$, and $V_{0,\mathrm{HPP}}=123.0\pm0.1$ Å^3/three-iodine atoms. For comparison also illustrated in Fig. 5 is an extrapolation of the equation of state reported by Reichlin *et al.*[19] for iodine having a high-pressure form of the fcc structure, where the volume of $(3/4)V_{\mathrm{fcc-iodine}}$ is plotted. The molar volume of the HPP of BI_3 is distinctly larger than that of the fcc I_2 by ~24% at 10 GPa and ~16% at 45 GPa, indicating the presence of boron atoms somewhere within the fcc lattice of iodine atoms.

C. Structural evolution on approaching to the phase transition

Values of two positional parameters of the iodine atom in the hexagonal structure, x and y, decrease almost linearly with increasing pressure from 0.039 and 0.357 at 1 atm (Ref. 9) to 0.0133 and 0.3326 at 5.9 GPa, respectively. Distances between the ith and the jth iodine atoms, r_{ij} (indices being given in Fig. 1), were calculated from the results of fitting and plotted in Fig. 6. The nearest neighbor distance $r_n=a_{\mathrm{fcc}}/\sqrt{2}$ is plotted in the HPP. The intramolecular distance r_{21} slightly increases with increasing pressure, indicating the weakening of covalent bonds between the boron and the iodine atom and the strengthening of intermolecular interactions. In fact, the atomic distances between different molecules decrease steeply under compression. This observation is consistent with marked hardening of Raman frequencies of the lattice modes.[10]

The phase transition to the HPP took place when one of the intermolecular distances, $r_{23'}$, became comparable to the intramolecular distance of r_{21} at ~6 GPa. The resulting fcc lattice of iodine atoms has the nearest neighbor distance approximately equal to the shortest distance in the hexagonal structure at the transition pressure. This coincidence demonstrates that the molecular layer of the hexagonal structure turns into the (111) close-packed layer of the fcc lattice. The HPP has a three-dimensional close-packed structure. Furthermore, its nearest-neighbor distance can become much shorter than the intramolecular I-I distance of ~3.66 Å at high pressures. Those facts are clear indications of monatomic character of the HPP.

D. Metallization and superconductivity

Pressure dependence of the electrical resistivity of BI_3 measured at room temperature is illustrated in Fig. 7. Rapid and continuous decrease in resistivity with increasing pressure ceases around 17 GPa, suggesting a change into a metallic state. The sample changed its color from transparent to opaque and a luster appeared on its surface above 20 GPa. No anomaly was detected at ~6 GPa where the sample underwent the structural transformation. Figure 8 represents the temperature dependence of the fractional resistance $R/R_{150\ \mathrm{K}}$ at some pressures at low temperature. When the temperature was lowered, the resistance was nearly independent of temperature up to 20 GPa. Small upturn of the curve below 20 K can be regarded as characteristic behavior of a semiconductor. This behavior disappeared at 23 and 27 GPa and the resistance shows apparently metallic temperature dependence.

Pressure induced a drastic drop in resistance below 1 K at 27 GPa as demonstrated in Fig. 9. This drop is considered to arise from an onset of the superconducting transition because the drop shifted to lower temperature by the application of magnetic fields (see the inset of Fig. 9). Reading the onset point of the drop, the transition temperature T_c was determined to be 0.5 K and T_c increased up to 2 K by further application of pressure to 65 GPa. The pressure variation in T_c for BI_3 is illustrated in Fig. 10 together with T_c for I_2 (Ref.

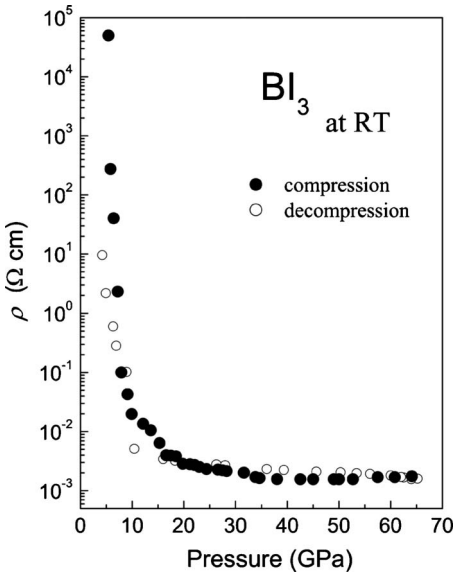

FIG. 7. Pressure variation in the electrical resistivity ρ in BI_3 at room temperature. Solid and open circles indicate ρ measured on compression and on decompression, respectively.

20) and SnI_4.[21] In BI_3, T_c increases significantly with increasing pressure and becomes nearly constant above 40 GPa.

IV. DISCUSSION

Let us consider the process of molecular dissociation at first. In the crystal structure at 1 atm, the molecular axis of the equilateral triangular BI_3 molecule, defined as the direction of the bond between the boron atom and the iodine atom with index 2 in Fig. 1, is not parallel to the a axis. The molecules at $z=1/4$ and $z=3/4$ are rotated, respectively, counterclockwise and clockwise by $\sim 2°$ around the boron atom in the basal planes. This configuration is being kept

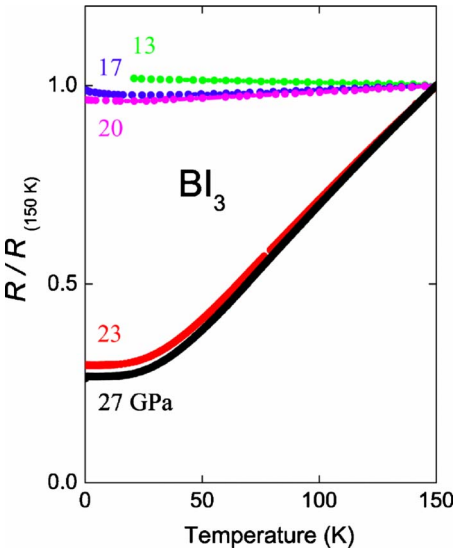

FIG. 8. (Color online) Fractional resistance $R/R_{150\ K}$ vs temperature in BI_3 at some pressures indicated in the figure.

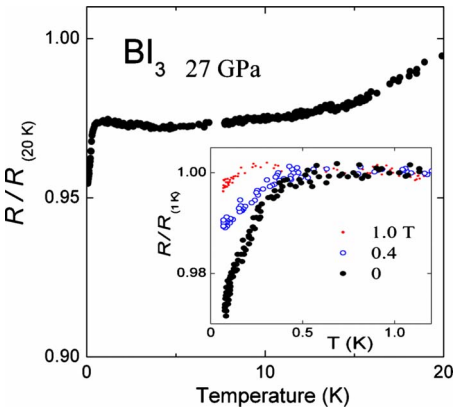

FIG. 9. (Color online) Fractional resistance $R/R_{20\ K}$ vs temperature in BI_3 at 27 GPa. The inset shows the effect of magnetic fields on the onset of the superconductivity at 27 GPa: 0 T (solid circle), 0.4 T (open circle), 1.0 T (dot).

unchanged during compression as expected from the observation in Fig. 6 that $r_{21'}$ and $r_{23'}$ do not tend to merge together. Symmetrization of a triangle formed by the iodine atoms of $i=1',2,3'$ does not proceed during compression, although shortening of those distances results in an increase in bond angle I(1′)-I(2)-I(3′), which approaches to 60° with increasing pressure as illustrated in Fig. 11. The phase transition, however, takes place before the angle reaches 60°, when $r_{23'}$ becomes equal to r_{21}, that is, the iodine atoms aligned at regular intervals form polymeric linear chains. Therefore, we conclude that a key trigger which induces the molecular dissociation and the phase transition in BI_3 is the equalization of the strength of the shortest intermolecular I-I bond with that of the intramolecular I-I bond within the molecular layer.

The process of the molecular dissociation in BI_3 is somewhat similar to that in iodine. Diatomic molecules of I_2 with covalent bond length of 2.75 Å form base-centered orthorhombic crystal structure consisting of stacked molecular layers. The molecular dissociation develops in the layer in

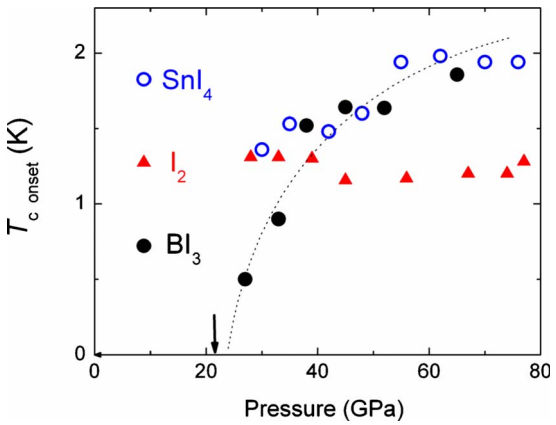

FIG. 10. (Color online) Pressure dependence of the superconducting transition temperature T_c in BI_3(solid circle), I_2 (triangle, Ref. 20) and SnI_4 (open circle, Ref. 21). The arrow indicates the pressure where the absence of superconductivity of BI_3 has been confirmed down to 35 mK. Dotted line is eye guide for T_c in BI_3.

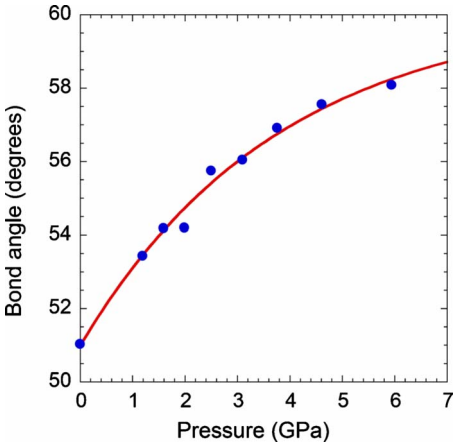

FIG. 11. (Color online) Variation in the bond angle I(1′)-I(2)-I(3′) with increasing pressure toward the transition pressure of 6.2 GPa. The structural change occurs before the angle reaches 60°. The curve is the guide to the eyes.

such a way that the intermolecular distances decrease and approach to the intramolecular bond length by compression, as in the case of BI_3. In the monatomic phase stabilized above 21 GPa, the bond length is elongated to 2.90 Å.[22] This 5.5% increment in length is taken as evidence of the molecular dissociation. Recent x-ray diffraction study of I_2 under hydrostatic condition by Takemura *et al.*[23] revealed that the fluctuation of the distances occurs in the range 2.86–3.11 Å in an intermediate incommensurate phase stabilized between 23 and 26 GPa prior to the molecular dissociation. The appearance of such fluctuation seems to be a natural consequence of competition among the intramolecular and the intermolecular forces with nearly equal strength. This might also happen in BI_3, although we detected no signs of the presence of such an intermediate state in this study. More detailed information will be provided by a hydrostatic experiment.

Molecules lose their identity in very different ways in other simple molecular iodides. In AsI_3, the isostructural transformation from the molecular to the ionic crystal takes place at the pressure where the intramolecular/intermolecular As-I distance ratio becomes about unity.[12] In the molecular phase of SnI_4, the shortest I-I distance between adjacent tetrahedral molecules reaches ~3.69 Å at 6.6 GPa, which is much smaller than the intramolecular I-I distance of ~4.31 Å, before the transition to the second crystalline phase at ~7.2 GPa.[17] This structural change is immediately followed by amorphization. From results of a x-ray absorption fine-structure study,[24] the molecular dissociation, which can be defined as distortion of the tetrahedral molecule due to elongation of the covalent Sn-I bond length, is inferred to occur at ~9 GPa in the state where the amorphous structure of polymeric network of distorted tetrahedra coexists with the remnant first and second crystalline phases.

Secondary, let us discuss crystal structure of the HPP. The present x-ray study was not capable of showing direct evidence of existence of the BI_3 molecules after the reverse phase transition. What we observed was that symmetry of the recovered crystal structure and measured values of the lattice constants well agree with those of the original hexagonal structure. This strongly supports the view that the molecules are restored at the reverse transition. It was also observed that the magnitude of pressure hysteresis of the transition is as small as ~1 GPa. We infer from those observations that displacements of the boron atoms associated with the structural change are rather small.

Most likely interstitial positions in the fcc structure are octahedral and tetrahedral sites. Estimation of their radii, r_o and r_t, in fcc I_2 from the interpolated equation of state shown in Fig. 5 yielded r_o=0.697 Å and r_t=0.378 Å at 7.0 GPa and r_o=0.634 Å and r_t=0.349 Å at 46.1 GPa. According to Shannon,[25] the ionic radii of B^{3+} with six coordinate and with four coordinate are 0.41 Å and 0.25 Å, respectively. Thus both sites are large enough to accommodate the B^{3+} ions. The tetrahedral site is smaller than the octahedral site but much closer to the position where the boron atom is located in the molecular phase. Although it is difficult for us to suggest a definite crystal structure of the HPP of BI_3 from above consideration, the model that the boron atoms randomly occupy tetrahedral sites in the fcc lattice of the iodine atom seems acceptable.

Finally, we discuss electrical properties of BI_3 at high pressure. The metallization of BI_3 occurs at 23 GPa at which the lattice constant of the fcc lattice is estimated to be 4.879 Å. A first-principles calculation of electronic band structure for iodine with the fcc structure having much larger lattice constant of 5.429 Å demonstrated that it still remains in a metallic state.[26] This result suggests that the conduction in the monatomic phase of BI_3 is strongly suppressed by the presence of boron atoms. Further theoretical consideration will elucidate the mechanism of metallization in BI_3.

Comparison of superconductive properties of I_2, BI_3, and SnI_4 in Fig. 10 shows that the transition appears at nearly the same pressure around 25 GPa in these materials and their maximum values of T_c lie within a very limited temperature range 1.3–2.0 K. From the viewpoint of crystal structure, each substance has a different structure from others at a pressure where the superconductivity is initially induced. In BI_3, the high-pressure monatomic phase becomes superconductive at 27 GPa. Iodine has an incommensurate structure at 22 GPa and SnI_4 has the amorphous form characterized by dense random packing of tin and iodine atoms at ~25 GPa.[27] Although all three structures may be regarded as minor modifications of the close packed arrangement of atoms, it is rather difficult to address a specific structural feature which can account for similarities in superconductive properties. We also see negative correlation between metallization and crystal structure in those systems. Boron triiodide becomes metallic at 23 GPa in the monatomic phase, I_2 at 16 GPa in the molecular phase and SnI_4 at 12 GPa in the amorphous phase coexistent with crystalline phases. Such a comparison demonstrates that the differences in dimensionality of the molecular shape introduces different type of anisotropy of crystal structure and thus results in a variety of response of crystal structure and electrical properties to pressure. It is to be pointed out that most of those experimental results were obtained from measurements under nonhydrostatic pressure and thus in different shear stress and strain conditions. Hydrostatic condition is crucial for future works

to make more substantial comparisons of structural and electrical properties at high pressure.

V. CONCLUSIONS

We carried out x-ray diffraction and electrical resistivity measurements of a highly anisotropic molecular crystal of BI_3 at high pressure. A new reversible phase transition from the molecular phase to the monatomic phase with the fcc lattice of iodine atoms was observed to occur at 6.2 ± 0.2 GPa. This first-order phase transition is characterized by the continuous densification in the molecular layer and the discontinuous crush of stacking of the layers. The reverse transition took place at 5.0 ± 0.2 GPa. Metallization takes place at 23 ± 1 GPa in the monatomic phase and superconductive transition appears at 27 ± 1 GPa. Comparison of the process of molecular dissociation and the electronic properties of BI_3 with iodine and other simple molecular iodides shows that each material exhibits quite different response of crystal structure and electronic properties to compression.

ACKNOWLEDGMENTS

Part of this work was performed at SPring-8 under the approval of the Japan Synchrotron Radiation Research Institute, Proposals No. 2003B0413ND and No. 2004A0124ND and by the Scientific Research (S), 19104009 and Global COE Program (Core Research and Engineering of Advanced Materials-Interdisciplinary Education Center for Materials Science), MEXT, Japan.

*hamaya.nozomu@ocha.ac.jp

[1] R. J. Hemley, Annu. Rev. Phys. Chem. **51**, 763 (2000), and references therein.
[2] M. Ross, Nature (London) **292**, 435 (1981).
[3] E. Wigner and H. B. Huntington, J. Chem. Phys. **3**, 764 (1935).
[4] D. A. Young, *Phase Diagrams of the Elements* (California University Press, Berkley, 1991), p. 56.
[5] Y. Fujii, M. Kowaka, and A. Onodera, J. Phys. C **18**, 789 (1985).
[6] N. Hamaya, K. Sato, K. Usui-Watanabe, K. Fuchizaki, Y. Fujii, and Y. Ohishi, Phys. Rev. Lett. **79**, 4597 (1997).
[7] M. P. Pasternak, R. D. Taylor, M. B. Kruger, R. Jeanloz, J. P. Itie, and A. Polian, Phys. Rev. Lett. **72**, 2733 (1994).
[8] A. L. Chen, P. Y. Yu, and M. P. Pasternak, Phys. Rev. B **44**, 2883 (1991).
[9] B. Albert and K. Schmitt, Z. Anorg. Allg. Chem. **627**, 809 (2001).
[10] A. Anderson and J. Lauren Lettress, J. Raman Spectrosc. **33**, 173 (2002).
[11] J. Trroter and T. Zobel, Z. Kristallogr. **123**, 67 (1966).
[12] H. C. Hsueh, R. K. Chen, H. Vass, S. J. Clark, G. J. Ackland, W. C.-K. Poon, and J. Crain, Phys. Rev. B **58**, 14812 (1998).
[13] H. K. Mao, P. M. Bell, J. W. Shaner, and D. J. Steinberg, J. Appl. Phys. **49**, 3276 (1978).
[14] F. Izumi and T. Ikeda, Mater. Sci. Forum **321-324**, 198 (2000).
[15] K. Shimizu, K. Amaya, and N. Suzuki, J. Phys. Soc. Jpn. **74**, 1345 (2005).
[16] P. Vinet, J. Ferrante, J. R. Smith, and J. H. Rose, J. Phys. C **19**, L467 (1986).
[17] K. Sato and N. Hamaya, Rev. High Pressure Sci. Technol. **7**, 278 (1998).
[18] E.-Fr. Düsing, W. A. Grosshans, and W. B. Holzapfel, J. Phys. Colloq. **45**, C8-203 (1984).
[19] R. Reichlin, A. K. McMahan, M. Ross, S. Martin, J. Hu, R. J. Hemley, H. K. Mao, and Y. Wu, Phys. Rev. B **49**, 3725 (1994).
[20] K. Shimizu, N. Tamitani, N. Takeshita, M, Ishizuka, K. Amaya and S. Endo, J. Phys. Soc. Jpn. **61**, 3853 (1992).
[21] N. Takeshita, S. Kometani, K. Shimizu, K. Amaya, N. Hamaya, and S. Endo, J. Phys. Soc. Jpn. **65**, 3400 (1996).
[22] K. Takemura, S. Minomura, O. Shimomura, Y. Fujii, and J. D. Axe, Phys. Rev. B **26**, 998 (1982).
[23] K. Takemura, K. Sato, H. Fujihisa, M. Onoda, Nature (London) **423**, 971 (2003).
[24] F. Wang and R. Ingalls, in *High Pressure Science and Technology*, edited by W. A. Trzeciakowski (World Scientific, Singapore, 1996), p. 289.
[25] R. D. Shannon, Acta Crystallogr., Sect. A: Cryst. Phys., Diffr., Theor. Gen. Crystallogr. **32**, 751 (1976).
[26] H. Fujihisa (private communications).
[27] A. Ohmura, K. Sato, N. Hamaya, M. Isshiki, and Y. Ohishi, Phys. Rev. B **80**, 054201 (2009).